HHS Public Access

Author manuscript

*Cell*. Author manuscript; available in PMC 2019 March 22.

Published in final edited form as:

*Cell*. 2018 March 22; 173(1): 130–139.e10. doi:10.1016/j.cell.2018.02.017.

# A circadian clock in the blood-brain barrier regulates xenobiotic efflux

**Shirley L. Zhang**[1], **Zhifeng Yue**, **Denice M. Arnold**, **Gregory Artiushin**, and **Amita Sehgal**[1,*]

Chronobiology Program at Penn and Howard Hughes Medical Institute, Perelman School of Medicine at the University of Pennsylvania, Philadelphia, PA, 19104, USA

[1]Center for Sleep and Circadian Neurobiology, Perelman School of Medicine at the University of Pennsylvania, Philadelphia, PA, 19104, USA

## Summary

Endogenous circadian rhythms are thought to modulate responses to external factors, but mechanisms that confer time-of-day differences in organismal responses to environmental insults/therapeutic treatments are poorly understood. Using a xenobiotic, we find that permeability of the *Drosophila* "blood"-brain barrier (BBB) is higher at night. The permeability rhythm is driven by circadian regulation of efflux and depends upon a molecular clock in the perineurial glia of the BBB, although efflux transporters are restricted to subperineurial glia (SPG). We show that transmission of circadian signals across the layers requires gap junctions, which are expressed cyclically. Specifically, during nighttime gap junctions reduce intracellular magnesium ($[Mg^{2+}]i$), a positive regulator of efflux, in SPG. Consistent with lower nighttime efflux, nighttime administration of the anti-epileptic phenytoin is more effective at treating a *Drosophila* seizure model. These findings identify a novel mechanism of circadian regulation and have therapeutic implications for drugs targeted to the central nervous system.

## In Brief

The circadian clock influences the permeability of the blood-brain barrier, affecting drug efficacy at different times of day.

[*]Correspondence to/lead contact: amita@pennmedicine.upenn.edu.

**Declaration of Interests:** The authors have no financial conflicts to disclose.

**Author Contributions:**

Conceptualization, S.L.Z. and A.S.; Methodology, S.L.Z., Z.Y., A.S.; Investigation, S.L.Z., Z.Y., D.M.A., and G.A.; Writing – Original Draft S.L.Z., and A.S.; Writing – Review & Editing S.L.Z., G.A., and A.S.; Funding Acquisition, S.L.Z. and A.S.

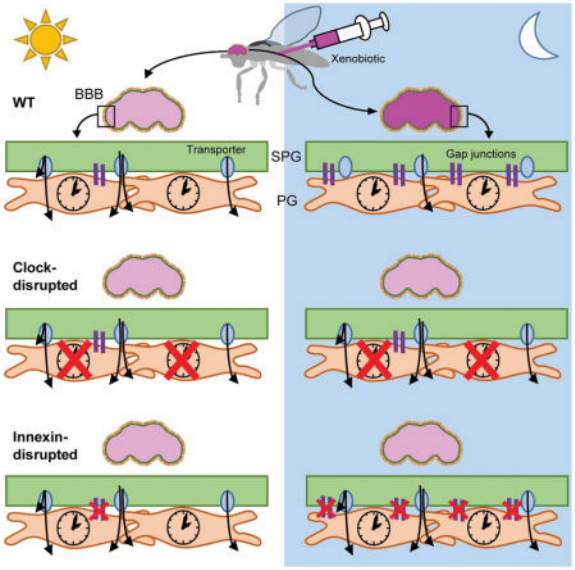


## Introduction

Circadian rhythms are endogenous, entrainable oscillations of biological processes that are dependent on a molecular clock. The central clock that drives rhythmic behavior is located in the brain, but clocks are also found in peripheral tissues where they exert local control over physiological functions (Ito and Tomioka, 2016; Mohawk et al., 2012). Peripheral clocks share largely the same core clock machinery as the central clock, but target tissue-specific genes, generating rhythms in many different physiological processes. Rhythms are observed in behaviors such as sleep, secretion of many hormones, lipid and glucose metabolism as well as lung and cardiac function, to mention just a few examples (Mohawk et al., 2012). Given the pervasive nature of circadian rhythms, it is generally thought that the response of an organism to drugs and therapies must also vary with time of day (Dallmann et al., 2016; Kaur et al., 2016). To date, the mechanisms suggested for such responses include rhythmic expression of molecular targets and/or rhythms in the responsiveness of the target tissue (Antoch et al., 2005).

A key obstacle for therapeutic drugs administered for the treatment of CNS disease is passage through the blood brain barrier (Abbott, 2013). Higher concentrations of drug facilitate entry, but efficacy is limited by dose-dependent toxicity of peripheral tissues; thus, many researchers have been engineering methods to improve drug delivery to the CNS (Banks, 2016). The BBB in mammals consists of blood vessels surrounded by endothelial tight junctions, which have many evolutionarily conserved adhesion and transport molecules (Ballabh et al., 2004). Although *Drosophila* have an open circulatory system, they also have a barrier between the hemolymph, insect “blood”, and the brain, which is structurally and functionally similar to the mammalian BBB (DeSalvo et al., 2011, 2014). The *Drosophila* BBB consists of a contiguous, flattened layer of subperineurial glia (SPG) and perineurial glia (PG) that covers the entire central nervous system. The cells of the SPG have extensive contact zones in which septate junctions prevent molecules from paracellular diffusion,

similar to the mechanism found in mammalian BBB endothelial cells (Limmer et al., 2014). In addition, *Drosophila* BBB cells interact via structurally and functionally conserved gap junctions, resembling those connecting astrocyte and endothelial cell components of the mammalian BBB (Abbott et al., 2006; Skerrett and Williams, 2017). Transport of molecules through the *Drosophila* BBB uses many of the same mechanisms as in the mammalian BBB, including homologous membrane transport protein families such as the ATP-binding cassette (ABC) transporter family, which includes p-glycoprotein (pgp) (DeSalvo et al., 2014; Hindle et al., 2017; Mayer et al., 2009). The similarity of BBB layers in vertebrates and invertebrates strengthens the idea that BBB mechanisms are conserved, suggesting that novel findings in invertebrate model organisms will have a significant impact on our understanding of vertebrate BBB functions.

In this study, we examine xenobiotic permeability in *Drosophila* and find that it is dependent on a circadian clock in the BBB. We find that the circadian clock-containing cells (PG) of the BBB maintain oscillating gap junctions, which are required to regulate the intracellular concentration of magnesium ions ($[Mg^{2+}]i$) in the ABC-like transporter-containing SPG cells. The rhythm in BBB permeability produces a rhythm of drug accumulation in the brain, resulting in increased responsiveness of seizure-sensitive *Drosophila* to therapeutic drugs delivered at night. These results reveal a novel mechanism of circadian regulation and suggest that therapeutic drugs targeting the CNS should be given at optimal circadian times for BBB entry/retention to minimize the dosage and reduce toxic side effects.

## Results

### The blood-brain barrier contains a molecular clock that is required for a rhythm in xenobiotic retention

To determine whether permeability of drugs to the brain varies with time of day, we first examined whether the accumulation of rhodamine b (RHB), a xenobiotic, is different in iso31 (wild type) brains across the circadian day. We injected female flies with RHB in the thorax and determined the amount of drug in the brain after 1 hr. Although there was variability in the amount of RHB retained in the body across individual flies, the average amount of dye in the body was similar between time points (Figure S1a). To account for the differences in injections of individual flies, the amount of drug in the brain was normalized to the amount of drug remaining in the rest of the body for each fly. RHB fluorescence in the brain showed a trough during midday and a peak in the early night, demonstrating diurnal changes in permeability of the brain (Figure 1a). Using *period* null ($per^{01}$) flies, which are deficient in a core component of the molecular circadian clock, we found that the diurnal oscillation in drug retention was abolished (Figure 1b). To verify that the circadian cycle in permeability was not limited to RHB, we assayed daunorubicin, another pgp substrate (Masuyama et al., 2012), and found a similar rhythm (Figure S1b). These results show that permeability of the brain to xenobiotic drugs is dependent on the endogenous circadian clock.

In *Drosophila*, as in mammals, core clock components are present in many tissues other than the central brain clock neurons (Ito and Tomioka, 2016). We sought to determine whether the BBB has a functional molecular clock by examining expression of the clock protein,

PER, in the two groups of glia that constitute the *Drosophila* BBB. Thus, we expressed GFP in the BBB using PG-specific (*NP6293-GAL4*) and SPG-specific (*moody-GAL4*) drivers (Figure S1c) and looked for co-localization with PER. PER is undetectable in SPG cells (Figure S1d), but it is expressed rhythmically in PG cells, such that daily changes in its levels and subcellular localization are consistent with 24-hour oscillations of PER in the brain clock neurons (Figure 1c; Curtin et al., 1995; Ito and Tomioka, 2016). These data identify a molecular clock within the PG cells of the BBB. To determine whether the rhythm in permeability is dependent on the PG clock, we disrupted clock function specifically in PG cells. As the tools for tissue-specific ablation of PER are not very effective, we used a dominant-negative version of the *per* transcriptional activator, CYCLE (dnCYC) to disrupt the clock (Xu et al., 2008). Disrupting the circadian clock with a *dncyc* transgene in PG cells did not affect behavioral rhythms (Figure S1e), which are controlled by specific clock neurons in the brain (Peschel and Helfrich-Förster, 2011). However, flies expressing *UAS-dncyc* under the control of PG-*GAL4* no longer display nighttime increases of RHB retention in the brain compared to the genetic controls (Figure 1d), suggesting that the PG clock is necessary for the circadian rhythm of permeability. We also expressed *UAS-dncyc* under the control of the SPG-*GAL4* and found no change in the rhythm of RHB permeability (Figure 1e), consistent with the absence of a molecular circadian clock in the SPG. PG-*GAL4* and SPG-*GAL4* controls were rhythmic (Figure S1f–g).

## Cyclic efflux, regulated non-cell-autonomously by the circadian clock, underlies the rhythm in BBB permeability

To determine the mechanisms that drive rhythms of permeability, we assessed RHB in *Drosophila* brains ex-vivo. Brains were dissected, incubated in RHB, and immediately imaged with a confocal microscope following removal of the RHB solution. The amount of RHB in the brains in the first frame was similar between dead flies and live flies, showing that influx of RHB into the brain is via a passive mechanism (Figure S2a left panel). Further, similarity in initial fluorescence between brains at zeitgeber time (ZT) 4–8 (ZT0=lights on and ZT12=lights off) compared to ZT12-16 suggests negligible time-of-day differences in influx (Figure S2a right panel). Photo-bleaching and passive diffusion from the brain were controlled using the loss in fluorescence of dead fly brains; however, even after controlling for these factors, the level of drug in the live brains declined over an 8 minute period. The loss of drug was greater in the brains during the daytime, ZT4-8, compared to early nighttime, ZT12-16 (Figure 2a). The decline in brain RHB during the daytime was blunted in null mutants of MDR65, the major RHB efflux transporter, suggesting that the daytime reduction is due to active efflux by pgp-homologous transporters (Figure 2a). Further, when we used verapamil to inhibit pgp-homologous transporters in wild type flies, we also found a reduction in RHB loss at in ZT4-8, but not at ZT12-16 (Figure S2b), presumably because efflux is already low at this time. Higher efflux during the day is consistent with lower permeability at this time, thereby providing a mechanism for the rhythm in permeability.

Using an antibody that recognizes a highly conserved region of pgp, we stained for transporter expression at the BBB and found colocalization with the SPG, but not the PG (Figure 2b). We then assessed the levels of pgp-like transporter expression in the *Drosophila* brain at different times of day, but did not detect obvious oscillations in either mRNA,

measured by qPCR of pgp-like transporters *mdr65* and *mdr49* (Figure S2c), or protein, assayed by immunofluorescence using the c219 anti-pgp antibody (Figure S2d). Together these results indicate that the PG clock does not regulate expression of pgp-like transporters. We hypothesize that the PG clock regulates the activity of pgp-like transporters present in the SPG.

## Cyclically-expressed gap junctions are required for the rhythm in BBB permeability

To determine how pgp transporters are regulated by a non-cell autonomous clock, we considered mechanisms by which SPG and PG cells might communicate with each other. As communication between barrier glia is thought to be mediated by gap junctions (Speder and Brand, 2014; Weisburg et al., 1991), we assessed a possible role for innexins. To examine innexin expression in isolated BBB cells, we used SPG-*GAL4* and PG-*GAL4* to drive *mCD8GFP* and separated dissociated brains by fluorescence-activated cell sorting (FACS); even 100 brains yielded very few cells, with less than 50 SPG cells recovered per brain (Figure S3a). Thus, we pooled samples from several time points across the day and measured mRNA levels in sorted glia (labeled using *Repo-GAL4* driving *mCD8GFP*), PG, or SPG populations and detected *Inx1* and *Inx2* expression in all cell types at or above total sorted brain levels (Figure S3b). To assess time-of-day differences in innexin (Inx) mRNA expression, we dissected whole brains and found that Inx1 (ogre) and Inx2 both cycle in wild type brains, but not in $per^{01}$ circadian clock mutants (Figure 3a–b). We also used immunofluorescence microscopy to measure expression of INX2 protein within the BBB (*9-137GAL4>mCD8GFP*) at different times of day. We quantified the mean level of INX2 fluorescence only where it colocalized with the BBB marker and found that it is expressed cyclically; however, surprisingly, the phase of the cycling is very different from that of the RNA (Figure 3c). We hypothesize that *Inx2* mRNA is expressed with a different phase in other glial populations and these, likely more abundant populations, determine the phase of the cycle in total brain mRNA. As described below, the phase of the INX2 protein cycling within the BBB is consistent with the mechanism we report here.

We next determined whether blocking innexins prevents time-of-day signals from the PG from reaching the SPG. Using an RNAi line previously reported to specifically knock down expression of *Inx1,* which is enriched in glia (Holcroft et al., 2013), we verified gene knock down by qPCR ((Speder and Brand, 2014); Figure S3c) and expressed it in PG cells. Assays of permeability revealed loss of rhythm and an overall decrease in nighttime RHB retention in PG-*GAL4>UAS-Inx1*$^{RNAi}$ *(gd)* flies relative to *GAL4* and *UAS* controls (Figure 3d). A second *Inx1*$^{RNAi}$ (TRiP) expressed in PG cells also exhibited arrhythmia in RHB permeability suggesting that the effect is not likely due to genetic background (Figure S3d). Since *Drosophila* gap junctions rarely form homotypic channels (Phelan and Starich, 2001), we examined whether inhibiting INX2 would also block oscillation of RHB permeability. As only one RNAi line was available for *Inx2* and was lethal when expressed in all glial cells, we expressed a dominant-negative form of INX2 (*UAS-dnInx2RFP*) (Speder and Brand, 2014) using the PG-*GAL4* driver. Inhibition of INX2 also resulted in loss of rhythmicity relative to controls (Figure 3e). Together these data suggest that gap junctions INX1 and INX2 are required in PG cells for the oscillation of RHB efflux in the SPG. Thus, connectivity of the PG and SPG via gap junctions appears to be important for relaying time-

of-day signals. We further verified the requirement for this connectivity by inhibiting gap junctions in the SPG, predicting that loss of gap junctions in the SPG would also block intercellular communication. Indeed when we used SPG-*GAL4* to drive *dnInx2*, we found a similar loss of the RHB permeability rhythm (Figure 3f).

As genetic manipulations of innexins could affect BBB functions by disrupting septate junctions, we first analyzed the septate junction protein Dlg1 by confocal microscopy and found that expression on the surface of SPG cells in mutant flies was grossly similar to that in wild type in (Figure 3Se). These results are consistent with previous work, which showed that manipulating innexins did not affect septate junctions in *Drosophila* larvae (Speder and Brand, 2014). To test the septate junctions functionally, we performed a dextran-dye penetration experiment (Pinsonneault et al., 2011). We found that the innexin mutant lines and controls were indistinguishable following injection of 10kd dextran dye into the hemolymph indicating that septate junctions are intact (Figure 3Sf).

## Gap junctions drive cycling of intracellular magnesium concentrations in the SPG

The requirement for gap junctions suggested involvement of a small second messenger that could diffuse through these channels. Higher levels of $[Mg^{2+}]$i are known to increase pgp transporter activity (Booth et al.; Shapiros and Ling, 1994), while increasing intracellular calcium ion concentration ($[Ca^{2+}]$i) is thought to inhibit pgp activity (Liang and Huang, 2000; Thews et al., 2006). We initially assessed $[Mg^{2+}]$i and $[Ca^{2+}]$i in both the PG and SPG using a pan-BBB driver (9-137-*GAL4*). For $[Mg^{2+}]$i detection, we used the ratiometric fluorescent indicator MagFura2 and measured mean fluorescent intensity by flow cytometry (Figure S4a). We found that the $[Mg^{2+}]$i levels in the BBB, labeled by 9-137-*GAL4* driving *mCD8GFP*, cycle with a zenith at ZT2 and nadir at ZT14 (Figure S4b). For measurements of $[Ca^{2+}]$i, we used 9–137 to drive an NFAT-based sensor, CaLexA (calcium-dependent nuclear import of Lex A) (Masuyama et al., 2012). This driver resulted in high specific expression of the CaLexA reporter with nearly an absence of background noise in the *Drosophila* brain, allowing for quantification of the fluorescence images with a confocal microscope. We measured CaLexA signals across the circadian day and found an opposing rhythm to $[Mg^{2+}]$i (Figure S4c). Importantly, the phase of these $[Mg^{2+}]$i and $[Ca^{2+}]$i oscillations is consistent with high efflux transporter activity during the day.

To address the dynamics of the ions in the subsets of the BBB, we labeled either the PG (PG-*GAL4>UAS-mCD8RFP*) or the SPG (SPG-*GAL4>UAS-mCD8RFP*) and measured both magnesium and calcium in the same brain sample, using Magfura2 along with the $[Ca^{2+}]$i indicator Cal630. In addition, we assessed the effect of junctional communication on ionic concentrations. Thus, control brains or brains containing PG-*GAL4>UAS-dnInx2RFP* or SPG-*GAL4>UAS-dnInx2RFP* were incubated with the ion indicators and analyzed by flow cytometry. Interestingly, while control SPG had comparable levels of ions to the PG, inhibiting INX2 function resulted in higher $[Mg^{2+}]$i and lower $[Ca^{2+}]$i in the SPG compared to PG (Figure 4a). Because efflux transporters regulated by magnesium/calcium ions are located in the SPG, we initially focused our efforts on this layer and found that $[Mg^{2+}]$i is cyclic, peaking early in the day and dropping at night (Figure 4b); however, no obvious cycle was observed in $[Ca^{2+}]$i in the SPG (Figure S4d). These data suggested that although

both ions cycle in the BBB, $[Mg^{2+}]i$ is the more likely candidate in affecting transporters in the SPG. Uncoupling the transporter-containing SPG from the clock-containing PG using dnInx2 (SPG-*GAL4>UAS-dnInx2RFP*) abolished the cycling of $[Mg^{2+}]i$ in the SPG (Figure 4c). We also examined $[Mg^{2+}]i$ in the PG at different times of day, in the presence and absence of gap junctional communication with SPG cells. Although we did not detect a cycle in the PG under either condition, we found that $[Mg^{2+}]i$ was highest at ZT14 when junctional communication was intact (Figure 4d); however, when PG cells were genetically uncoupled from the SPG (PG-*GAL4>UAS*-dnInx2RFP), $[Mg^{2+}]i$ at ZT14 was low (Figure 4e). We suggest that the PG acts as a sink at ZT14, draining $[Mg^{2+}]i$ from the SPG through gap junctions. Together these data indicate that junctional communication equilibrates ionic concentrations across the two layers; specifically, increased communication at night lowers magnesium in the SPG to reduce efflux transport and promote permeability.

## Drug-mediated recovery from seizures is dependent on the BBB clock

Since permeability of the BBB is dependent on the circadian clock, it seemed logical that the effect of xenobiotic neuromodulatory drugs would also follow a rhythmic pattern based on how much drug is retained in the brain. To test this idea, we fed an anti-seizure xenobiotic drug, phenytoin, to *easily-shocked (eas)* mutant flies, which are sensitive to seizures induced by mechanical stimuli. Following 2 hrs of feeding on drug-containing media, the *eas* mutants were vortexed and the number of flies paralyzed or seizing was recorded every 15 secs and the average latency to recovery was calculated for each vial of flies at each time point. Overall, *eas* mutants receiving phenytoin recover faster and so their latency to recovery is lower as compared to flies receiving vehicle (Figure 5a). We calculated the effect of the drug on recovery latency at different times of day, and found an increase in drug efficacy at night (Figure 5b), which is consistent with the rhythm of BBB permeability we report here. While there was some variability in the amount of phenytoin ingested by individual flies as measured by blue food dye intake, there was no significant difference among time points (Figure S5). We infer that the increased efficacy of the drug at night results from decreased pgp-mediated efflux, which increases nighttime retention and thereby enhances neuromodulatory effects.

To determine whether the time-of-day-specific response of *eas* mutants to phenytoin was due to the circadian clock in the BBB, we introduced the PG-*GAL4* driver along with *UAS dncyc* into the *eas* mutants. Unfortunately, this genetic manipulation altered the threshold of seizure sensitivity and decreased the penetrance of the *eas* phenotype within the population at baseline and therefore the magnitude of the drug-dependent change in recovery is not directly comparable to the original *eas* mutants. Nonetheless, we assessed whether there were time-of-day differences in the response of *eas* mutants to phenytoin in the absence of the PG clock (Figure 5c). Importantly, we found that there were no circadian differences in drug response in the absence of the PG clock (Figure 5d). These results indicate the clock in the BBB drives a rhythm in phenytoin-induced effects on the brain.

## Discussion

We report here a rhythm of BBB permeability driven by a clock within the BBB, but through a novel non-cell-autonomous mechanism. These findings, which are the first to demonstrate a circadian rhythm in BBB permeability, could account for previous findings of daily fluctuations in drug/hormone expression in the brain. For instance, levels of leptin and cytokines were found to differ between the blood and the cerebrospinal fluid at different times of day (Pan and Kastin, 2001; Pan et al., 2002). In addition, the level of quinidine, a pgp-effluxed drug, in the rat brain depends on the timing of administration, with much lower levels of quinidine in the brain during the animals' active period (Kervezee et al., 2014). We find that pgp function is regulated by the BBB clock to efflux at a higher rate during the daytime, which is the active period of the fly, thus reducing the level of drug in the brain. Similar regulation in the rat would account for the time-of-day changes in brain levels of quinidine. Humans are diurnal, like flies, and so the human BBB would presumably display the same phase of efflux as that observed in *Drosophila*.

Our results suggest that the molecular clock in the PG cells controls rhythms of INX1 and INX2, which regulate $[Mg^{2+}]i$ levels within the SPG, thereby producing a cycle in the activity of the pgp transporters. Due to the high levels of $[Mg^{2+}]i$ in uncoupled SPG, we suggest that connectivity of the SPG to the PG via gap junctions provides a sink for $[Mg^{2+}]i$, reducing the availability of $[Mg^{2+}]i$ for transporter activity (Figure 6). This is supported by the $[Mg^{2+}]i$ profile in the PG cells, in particular at ZT14 when they show low $[Mg^{2+}]i$ levels unless they are connected to the SPG, whereupon levels are quite high. It is also consistent with the phase of INX2 cycling in the BBB, which shows a peak coincident with the lowest levels of $[Mg^{2+}]i$ within the SPG. It will be interesting to determine whether gap junctions connecting astrocytes to endothelial cells perform a similar function in the mammalian BBB. The finding that $[Mg^{2+}]i$ couples circadian clocks to transporter activity in the *Drosophila* BBB also provides an important role for magnesium in circadian physiology in animals. Daily fluctuations in $[Mg^{2+}]i$ have been found to regulate cellular processes in mammalian cell culture and single-celled algae (Feeney et al., 2016).

It is interesting that flies use non-cell autonomous mechanisms to drive a rhythm of BBB permeability, and fits with the idea that clocks localize to specific cell populations in *Drosophila* and control behavior/physiology through circuits (Chatterjee and Rouyer, 2016; Guo et al., 2014; Liang et al., 2017). However, given that one class of *Drosophila* BBB cells contains clocks, these findings still raise the question of why clocks and transporters localize to different cell types. We speculate that the two BBB layers have distinct functions that require different types of regulation and activity. Indeed, BBB glia in *Drosophila* have recently been implicated in functions other than regulation of the barrier, for instance in metabolic functions relevant for the brain (Volkenhoff et al., 2015). Given the generally strong circadian influence in metabolic physiology, it is possible that the clock is located in PG cells to directly control metabolic activity, while the transporters need to be isolated from such processes.

While circadian studies have historically focused on neurons, glia have recently been gaining attention for their contribution to the generation/maintenance of rhythms

(Brancaccio et al., 2017; Damulewicz et al., 2013; Jackson et al., 2015; Tso et al., 2017). However, the rhythms assayed in most of these cases are those of behavioral locomotor activity and the relevant glia are usually astrocytes (Brancaccio et al., 2017; Jackson et al., 2015). The role we report here for BBB glia indicates more general regulation of circadian physiology by glia.

(Xie et al., 2013) demonstrated that amyloid beta is cleared from the brain via a glymphatic system during sleep. At first glance, these results may appear to contradict ours as they show increased clearance by the BBB during sleep while we demonstrate higher efflux during the day; however, their model examined an endogenous protein that is cleared largely by endocytic uptake followed by transcytosis (Yoon and Jo, 2012), rather than a xenobiotic subject to pgp-mediated efflux. Also, Xie et al examined the differences as a function of behavioral state rather than time-of-day. We suggest that these brain-clearing systems are entirely compatible. Since animals encounter xenobiotics primarily during their active period (i.e. through foraging, injury, etc), it would be evolutionarily advantageous to be poised to immediately expel the foreign particle; however, endogenous proteins or neurotoxins that slowly build up as a byproduct of brain functions during wakefulness may require a behavior shift to sleep in order for them to be cleared. Future work may resolve whether the circadian regulation of the BBB interacts with the sleep-dependent clearance of metabolites.

A major clinical implication of this work is the possibility of improving therapies with neuropsychiatric and neurological drugs. Chronotherapy aligns medical treatments to the body's circadian rhythms, taking into consideration circadian oscillations of the target tissue and rhythms in hormones, using the circadian information to minimize side effects and optimize outcomes (Dallmann et al., 2014). A study of epileptic patients unresponsive to standard doses of phenytoin and carbamazepine found that administration of all or most of the daily dose of medication at night improved seizure control (Yegnanarayan et al., 2006). Our results suggest a model in which the phase of BBB permissiveness is a key factor that determines therapeutic effects of xenobiotic drugs in the brain. In support of regulated efflux as the basis of BBB permeability, higher levels of pgp in humans correspond to a lack of responsiveness to seizure drugs (Loscher et al., 2011). Optimal timing of BBB transport and delivery of drugs can be equally or more important as the timing of CNS responsiveness and should be considered in administration of therapeutic regimens.

## STAR Methods

### Contact for Reagent and Resource Sharing

Further information and requests for resources and reagents should be directed to and will be fulfilled by the Lead Contact, Amita Sehgal (amita@pennmedicine.upenn.edu).

### Experimental Model and Subject Details

***Drosophila* lines—**Fly stocks were raised and maintained on cornmeal-molasses medium at 25°C. The $w^{1118}$ iso31 strain was used as wild type. When tested as controls, UAS and GAL4 fly lines were tested as heterozygotes after crossing to iso31. 5–14 day old adult female flies were used for experiments; the age range is further specified for each method.

## Method details

**Permeability in fly brains—**5–7 day old adult female flies were entrained to 12:12 LD cycles. RHB and daunorubicin delivery methods are similar to those previously described (Bainton et al., 2005). Briefly, a microinjection needle delivered intrahumoral 2.5 mg/mL RHB or 9 mg/ml daunorubicin in PBS between the posterior abdominal wall body segments of $CO_2$ anesthetized flies. Capillary action or positive pressure was applied to the needle under direct visualization over 1–2 secs to deliver an average volume of 50 nL per injection. Flies were given 1 hr after injection to rest and efflux the RHB at 25°C. Brains from the f lies were rapidly dissected in 1X PBS and washed with PBS before being placed in 50 μL 0.1% SDS. Brains were dissociated over >30 mins and the dye from brain samples was measured at excitation/emission: 540/590 using a Victor 3V (Perkin Elmer) plate reader. Bodies from the corresponding flies were homogenized, spun down and measured at the same wavelengths. Uninjected flies were used to adjust for background and the ratios of brain to body levels were calculated for individual flies for RHB and from 5 flies pooled for daunorubicin. Animals with less than 0.1 mg RHB detected in the body were excluded from analysis due to increased variability of the brain:body ratio at brain RHB detection threshold. Amount of RHB was calculated using a standard curve.

**Live imaging of fly brains RHB efflux—**Iso31 female flies were entrained to 12:12 LD cycles. Brains were carefully dissected in minimal hemolymph solution HL3.1 (Feng et al., 2004) (70mM NaCl, 5mM KCl, 4 $MgCl_2$mM, 10mM $NaHCO_3$, 5mM trehalose, 115 sucrose, and 5mM HEPES, pH 7.4) with forceps with care to minimize damage to the surface of the brain. Brains were incubated in RHB (125 μg/mL) with or without verapamil (100 μg/mL) for 2 mins and washed with HL3.1 media to image immediately. To determine the loss of fluorescence due to diffusion and photobleaching during imaging, flies were microwaved for 1 min prior to brain dissection. Brains were imaged for 10 mins using a Leica SP5 confocal microscope. FIJI software was used for analysis.

**Immunofluorescence microscopy—**Fly brains were dissected in cold PBS and fixed in 4% paraformaldehyde (PFA) for 10–20 min at room temperature. Brains were rinsed 3 × 10 min with PBS with 0.1% Triton-X (PBST), blocked for 30–60 min in 5% normal donkey serum or goat serum in PBST (NDST), and incubated overnight at 4°C in primary antibody diluted in NDST. Brains were then rinsed 4 × 10 min in PBST, incubated 2 hrs in secondary antibody diluted in NDST, rinsed 4 × 10 min in PBST, and mounted with Vectashield. Primary antibodies included guinea pig anti-PER UP1140 (1:1000), mouse anti-PGP C219 (10 μg/ml), and guinea pig anti-INX2 (1:1000), and guinea pig mouse anti-DLG1 (1:50). Secondary antibodies included goat anti-guinea pig Cy5 (Rockland), goat anti-guinea pig anti-AF555 (Jackson Immuno), donkey anti-mouse AF647 (Jackson Immuno). Brains were imaged using a Leica SP5 confocal microscope. FIJI software was used for analysis.

For dextran-dye penetration experiments, we injected fluorescence tagged 10000 molecular weight fixable dextran (25 mg/ml TMRD or 10 mg/ml AF647) into fly hemolymph under $CO_2$ anesthesia as previously described (Pinsonneault et al., 2011). 16–24 hours after injection, flies were anesthesized using $CO_2$ and decapitated. The proboscis was quickly removed from the head and the head was immediately submerged in 4% PFA for 15 min.

Following fixation, the brain was dissected and washed for < 4 × 10 min in PBST and mounted in Vectashield. Brains were imaged using a Leica SP5 confocal microscope.

**Rest:activity rhythms assays—**Locomotor activity assays were performed with the *Drosophila* Activity Monitoring System (Trikinetics) as described previously (Williams et al., 2001). 5–7-day-old female flies were entrained to a 12:12 LD cycle for 3 days then transferred to constant darkness for 5 days. Flies were maintained at 25°C throughout the assay.

**FACS sorting glial populations—**Brains were dissected in ice cold HL3.1 and were maintained on ice except during dissociation. Collagenase A and DNase I were added to final concentrations of 2 mg/mL and 20 μl/mL, respectively. Brains were dissociated at 37°C using a shaker at 2 50 rpm for 20 mins pausing at 10 mins to pipette vigorously. Dissociated tissue was filtered through 100 μm cell strainer and sorted using a 100 μm nozzle on a BD FACSAria (BD Biosciences). Dead cells were excluded with 4,6-diamidino-2-phenylindole (DAPI). Doublets were excluded using FSC-H by FSC-W and SSC-H by SSC-W parameters. $GFP^+$ cells gates were set using according to $GFP^-$ brain tissue. Data were analyzed using FlowJo version 10.3 (Tree Star).

**Quantitative PCR—**Brains were dissected in cold PBS and immediately lysed. RNA was extracted using RNeasy mini kit and reverse transcribed to cDNA using random hexamers and Superscript II (Invitrogen). Real-time polymerase chain reaction (PCR) was performed using Sybr Green PCR Master Mix (Applied Biosystems) with the oligonucleotides described in Table 2. Assays were run on ViiA7 Real-Time PCR system (Applied Biosystems). Relative gene expression was calculated using the ΔΔCt method normalizing to actin.

**Flow cytometric assay for intracellular magnesium and calcium levels—**Brains from entrained adult female flies (5–7 days) with fluorescently-labeled PG or SPG were dissected in adult hemolymph-like saline (AHL; 108mM NaCl, 5mM KCl, 2mM $CaCl_2$, 8.2mM $MgCl_2$, 4mM $NaHCO_3$, 1mM $NaH_2PO_4$-$H_2O$, 5mM trehalose, 10mM sucrose, 5mM HEPES; pH 7.5) on ice. Brains were brought to room temperature (RT) for 10 mins and incubated with 5 μM Magfura2-AM and 5 μM Cal630-AM for 20 mins at RT. Brains were washed with RT AHL for 3 × 5 mins. Then Collagenase IV and DNase I were added to final concentrations of 2 mg/mL and 20 units, respectively and brains were dissociated at 37°C with 250 rpm shaking for 15 mins. Dissociated tissue was filtered through 100 μm cell strainer and washed with FACS buffer (PBS with 1% w/v bovine serum albumin and 0.1% w/v sodium azide). Cells were analyzed on BD FACSCanto II (BD Biosciences). Doublets were excluded using FSC-H by FSC-W and SSC-H by SSC-W parameters. $RFP^+$ cells gates were set according to $RFP^-$ brain tissue. Data were analyzed using FlowJo version 10.3.

**Seizure recovery assay—**7–14 day old adult female $eas^{PC80}$ flies were starved for 24 hrs to allow for maximum drug dosing. Flies were given 5% sucrose and 1.5% agar with or without 0.6 mg/mL phenytoin a previously described dose to improve recovery from seizure (Reynolds et al., 2004). Flies were tested in 2 vials (1 control and 1 phenytoin), each containing 15 flies. Mechanical shock was delivered by vortexing flies at high speed for 5

secs. The assays were video recorded and the number of flies seizing was recorded at 15 sec intervals until the entire population had recovered. Recovery was defined as standing and was analyzed by a researcher blinded to the drug condition. Mean recovery time was calculated as the average time it took any individual fly to recover in a population. Flies that never seized were calculated as 0 secs for recovery time.

The blue dye feeding assay was performed as previously described (Deshpande et al., 2014). Briefly, after 24 hrs of starvation, flies were given food with 2% w/v FD&C Blue No. 1 for 2 hrs. Individual flies were homogenized and the absorbance at 620 nm was measured with a Victor 3V (Perkin Elmer) plate reader. The amount of food eaten was calculated by using a standard curve.

### Quantification and Statistical Analysis

The statistical details of experiments can be found in the figure legends. Circadian statistical analysis was performed in R using JTK_CYCLEv3.1. ANOVA and post-hoc Tukey tests were performed with GraphPad Prism. Student's T-tests were performed with Excel. Sample sizes were determined with powerandsamplesize.com.

## Supplementary Material

Refer to Web version on PubMed Central for supplementary material.

## Acknowledgments

This work was supported by grants T32HL07713 and R25MH060490 from the National Institutes of Health (S.L.Z.) and the Howard Hughes Medical Institute (A.S.). We thank Dr. John Hogenesch for assistance with statistical analysis and Dr. Annika Barber for assistance with visual representation of data.

## References

Abbott NJ. Blood-brain barrier structure and function and the challenges for CNS drug delivery. J Inherit Metab Dis. 2013; 36:437–449. [PubMed: 23609350]

Abbott NJ, Rönnbäck L, Hansson E. Astrocyte-endothelial interactions at the blood-brain barrier. Nat Rev Neurosci. 2006; 7:41–53. [PubMed: 16371949]

Antoch MP, Kondratov RV, Takahashi JS. Circadian clock genes as modulators of sensitivity to genotoxic stress. Cell Cycle. 2005; 4:901–907. [PubMed: 15917646]

Awasaki T, Lai SL, Ito K, Lee T. Organization and postembryonic development of glial cells in the adult central brain of Drosophila. J Neurosci. 2008; 28:13742–13753. [PubMed: 19091965]

Bainton RJ, Tsai LT, Schwabe T, DeSalvo M, Gaul U, Heberlein U. moody encodes two GPCRs that regulate cocaine behaviors and blood-brain barrier permeability in Drosophila. Cell. 2005; 123:145–156. [PubMed: 16213219]

Ballabh P, Braun A, Nedergaard M. The blood-brain barrier: an overview: structure, regulation, and clinical implications. Neurobiol Dis. 2004; 16:1–13. [PubMed: 15207256]

Banks WA. From blood-brain barrier to blood-brain interface: new opportunities for CNS drug delivery. Nat Rev Drug Discov. 2016; 15:275–292. [PubMed: 26794270]

Benzer S. From the gene to behavior. JAMA. 1971; 218:1015–1022. [PubMed: 4942064]

Booth CL, Pulaski L, Gottesman MM, Pastan I. Analysis of the Properties of the N-Terminal Nucleotide-Binding Domain of Human P-Glycoprotein.

Brancaccio M, Patton AP, Chesham JE, Maywood ES, Hastings MH. Astrocytes Control Circadian Timekeeping in the Suprachiasmatic Nucleus via Glutamatergic Signaling. Neuron. 2017; 93:1420–1435. e5. [PubMed: 28285822]

Chatterjee, A., Rouyer, F. Control of Sleep-Wake Cycles in Drosophila. 2016.

Curtin KD, Huang ZJ, Rosbash M. Temporally regulated nuclear entry of the Drosophila period protein contributes to the circadian clock. Neuron. 1995; 14:365–372. [PubMed: 7857645]

Dallmann R, Brown SA, Gachon F. Chronopharmacology: new insights and therapeutic implications. Annu Rev Pharmacol Toxicol. 2014; 54:339–361. [PubMed: 24160700]

Dallmann R, Okyar A, Levi F. Dosing-Time Makes the Poison: Circadian Regulation and Pharmacotherapy. Trends Mol Med. 2016; 22:430–445. [PubMed: 27066876]

Damulewicz M, Rosato E, Pyza E. Circadian regulation of the Na+/K+-ATPase alpha subunit in the visual system is mediated by the pacemaker and by retina photoreceptors in Drosophila melanogaster. PLoS One. 2013; 8:e73690. [PubMed: 24040028]

DeSalvo MK, Mayer N, Mayer F, Bainton RJ. Physiologic and anatomic characterization of the brain surface glia barrier of Drosophila. Glia. 2011; 59:1322–1340. [PubMed: 21351158]

DeSalvo MK, Hindle SJ, Rusan ZM, Orng S, Eddison M, Halliwill K, Bainton RJ. The Drosophila surface glia transcriptome: evolutionary conserved blood-brain barrier processes. Front Neurosci. 2014; 8:346. [PubMed: 25426014]

Deshpande SA, Carvalho GB, Amador A, Phillips AM, Hoxha S, Lizotte KJ, Ja WW. Quantifying Drosophila food intake: comparative analysis of current methodology. Nat Methods. 2014; 11:535–540. [PubMed: 24681694]

Feeney KA, Hansen LL, Putker M, Olivares-Yañez C, Day J, Eades LJ, Larrondo LF, Hoyle NP, O'Neill JS, van Ooijen G. Daily magnesium fluxes regulate cellular timekeeping and energy balance. Nature. 2016; 532:375–379. [PubMed: 27074515]

Feng Y, Ueda A, Wu CF. A modified minimal hemolymph-like solution, HL3.1, for physiological recordings at the neuromuscular junctions of normal and mutant Drosophila larvae. J Neurogenet. 2004; 18:377–402. [PubMed: 15763995]

Garbe DS, Fang Y, Zheng X, Sowcik M, Anjum R, Gygi SP, Sehgal A. Cooperative interaction between phosphorylation sites on PERIOD maintains circadian period in Drosophila. PLoS Genet. 2013; 9:e1003749. [PubMed: 24086144]

Guo F, Cerullo I, Chen X, Rosbash M. PDF neuron firing phase-shifts key circadian activity neurons in Drosophila. Elife. 2014; 3

Hindle SJ, Munji RN, Dolghih E, Gaskins G, Orng S, Ishimoto H, Soung A, DeSalvo M, Kitamoto T, Keiser MJ, et al. Evolutionarily Conserved Roles for Blood-Brain Barrier Xenobiotic Transporters in Endogenous Steroid Partitioning and Behavior. Cell Rep. 2017; 21:1304–1316. [PubMed: 29091768]

Holcroft CE, Jackson WD, Lin WH, Bassiri K, Baines RA, Phelan P. Innexins Ogre and Inx2 are required in glial cells for normal postembryonic development of the Drosophila central nervous system. J Cell Sci. 2013; 126:3823–3834. [PubMed: 23813964]

Hughes ME, Hogenesch JB, Kornacker K. JTK_CYCLE: an efficient nonparametric algorithm for detecting rhythmic components in genome-scale data sets. J Biol Rhythm. 2010; 25:372–380.

Ito C, Tomioka K. Heterogeneity of the Peripheral Circadian Systems in Drosophila melanogaster: A Review. Front Physiol. 2016; 7:8. [PubMed: 26858652]

Jackson FR, Ng FS, Sengupta S, You S, Huang Y. Glial cell regulation of rhythmic behavior. Methods Enzymol. 2015; 552:45–73. [PubMed: 25707272]

Kaur G, Phillips CL, Wong K, McLachlan AJ, Saini B. Timing of Administration: For Commonly-Prescribed Medicines in Australia. Pharmaceutics. 2016; 8

Kervezee L, Hartman R, van den Berg DJ, Shimizu S, Emoto-Yamamoto Y, Meijer JH, de Lange EC. Diurnal variation in P-glycoprotein-mediated transport and cerebrospinal fluid turnover in the brain. AAPS J. 2014; 16:1029–1037. [PubMed: 24917180]

Liang X, Huang Y. Intracellular Free Calcium Concentration and Cisplatin Resistance in Human Lung Adenocarcinoma A 549 Cells. Biosci Rep. 2000; 20

Liang X, Holy TE, Taghert PH. A Series of Suppressive Signals within the Drosophila Circadian Neural Circuit Generates Sequential Daily Outputs. Neuron. 2017; 94:1173–1189. e4. [PubMed: 28552314]

Limmer S, Weiler A, Volkenhoff A, Babatz F, Klambt C. The Drosophila blood-brain barrier: development and function of a glial endothelium. Front Neurosci. 2014; 8:365. [PubMed: 25452710]

Loscher W, Luna-Tortos C, Romermann K, Fedrowitz M. Do ATP-binding cassette transporters cause pharmacoresistance in epilepsy? Problems and approaches in determining which antiepileptic drugs are affected. Curr Pharm Des. 2011; 17:2808–2828. [PubMed: 21827408]

Masuyama K, Zhang Y, Rao Y, Wang JW. Mapping neural circuits with activity-dependent nuclear import of a transcription factor. J Neurogenet. 2012; 26:89–102. [PubMed: 22236090]

Mayer F, Mayer N, Chinn L, Pinsonneault RL, Kroetz D, Bainton RJ. Evolutionary conservation of vertebrate blood-brain barrier chemoprotective mechanisms in Drosophila. J Neurosci. 2009; 29:3538–3550. [PubMed: 19295159]

Mohawk JA, Green CB, Takahashi JS. Central and peripheral circadian clocks in mammals. Annu Rev Neurosci. 2012; 35:445–462. [PubMed: 22483041]

Pan W, Kastin AJ. Diurnal variation of leptin entry from blood to brain involving partial saturation of the transport system. Life Sci. 2001; 68:2705–2714. [PubMed: 11400913]

Pan W, Cornelissen G, Halberg F, Kastin AJ. Selected contribution: circadian rhythm of tumor necrosis factor-alpha uptake into mouse spinal cord. J Appl Physiol. 2002; 92:1357–62. discussion 1356. [PubMed: 11842079]

Peschel N, Helfrich-Förster C. Setting the clock - by nature: Circadian rhythm in the fruitfly *Drosophila melanogaster*. FEBS Lett. 2011; 585:1435–1442. [PubMed: 21354415]

Phelan P, Starich TA. Innexins get into the gap. BioEssays. 2001; 23:388–396. [PubMed: 11340620]

Pinsonneault RL, Mayer N, Mayer F, Tegegn N, Bainton RJ. Novel models for studying the blood-brain and blood-eye barriers in Drosophila. Methods Mol Biol. 2011; 686:357–369. [PubMed: 21082381]

Reynolds ER, Stauffer EA, Feeney L, Rojahn E, Jacobs B, McKeever C. Treatment with the antiepileptic drugs phenytoin and gabapentin ameliorates seizure and paralysis of Drosophila bang-sensitive mutants. J Neurobiol. 2004; 58:503–513. [PubMed: 14978727]

Shapiros AB, Ling V. THE JOURNAL OF BIOEGICAL CHEMISTRY ATPase Activity of Purified and Reconstituted P-glycoprotein from Chinese Hamster Ovary Cells*. 1994; 269:3745–3754.

Skerrett IM, Williams JB. A structural and functional comparison of gap junction channels composed of connexins and innexins. Dev Neurobiol. 2017; 77:522–547. [PubMed: 27582044]

Smendziuk CM, Messenberg A, Vogl AW, Tanentzapf G. Bi-directional gap junction-mediated soma-germline communication is essential for spermatogenesis. Development. 2015; 142:2598–2609. [PubMed: 26116660]

Speder P, Brand AH. Gap junction proteins in the blood-brain barrier control nutrient-dependent reactivation of Drosophila neural stem cells. Dev Cell. 2014; 30:309–321. [PubMed: 25065772]

Stork T, Engelen D, Krudewig A, Silies M, Bainton RJ, Klambt C. Organization and function of the blood-brain barrier in Drosophila. J Neurosci. 2008; 28:587–597. [PubMed: 18199760]

Thews O, Gassner B, Kelleher DK, Schwerdt G, Gekle M. Impact of extracellular acidity on the activity of P-glycoprotein and the cytotoxicity of chemotherapeutic drugs. Neoplasia. 2006; 8:143–152. [PubMed: 16611407]

Tso CF, Simon T, Greenlaw AC, Puri T, Mieda M, Herzog ED. Astrocytes Regulate Daily Rhythms in the Suprachiasmatic Nucleus and Behavior. Curr Biol. 2017; 27:1055–1061. [PubMed: 28343966]

Volkenhoff A, Weiler A, Letzel M, Stehling M, Klambt C, Schirmeier S. Glial Glycolysis Is Essential for Neuronal Survival in Drosophila. Cell Metab. 2015; 22:437–447. [PubMed: 26235423]

Weisburg WG, Barns SM, Pelletier DA, Lane DJ. 16S ribosomal DNA amplification for phylogenetic study. J Bacteriol. 1991; 173:697–703. [PubMed: 1987160]

Williams JA, Su HS, Bernards A, Field J, Sehgal A. A circadian output in Drosophila mediated by neurofibromatosis-1 and Ras/MAPK. Science (80- ). 2001; 293:2251–2256.

Xie L, Kang H, Xu Q, Chen MJ, Liao Y, Thiyagarajan M, O'Donnell J, Christensen DJ, Nicholson C, Iliff JJ, et al. Sleep drives metabolite clearance from the adult brain. Science (80-). 2013; 342:373–377.

Xu K, Zheng X, Sehgal A. Regulation of feeding and metabolism by neuronal and peripheral clocks in Drosophila. Cell Metab. 2008; 8:289–300. [PubMed: 18840359]

Yegnanarayan R, Mahesh SD, Sangle S. Chronotherapeutic dose schedule of phenytoin and carbamazepine in epileptic patients. Chronobiol Int. 2006; 23:1035–1046. [PubMed: 17050216]

Yoon SS, Jo SA. Mechanisms of Amyloid-β Peptide Clearance: Potential Therapeutic Targets for Alzheimer's Disease. Biomol Ther (Seoul). 2012; 20:245–255. [PubMed: 24130920]

Zeng H, Hardin PE, Rosbash M. Constitutive overexpression of the Drosophila period protein inhibits period mRNA cycling. EMBO J. 1994; 13:3590–3598. [PubMed: 8062834]

## Highlights

- The *Drosophila* BBB displays a circadian rhythm of permeability
- Cyclic efflux driven by a clock in the BBB underlies the permeability rhythm
- Circadian control is non-cell-autonomous via gap junction regulation of $[Mg^{2+}]i$
- An anti-seizure drug is more effective when administered at night

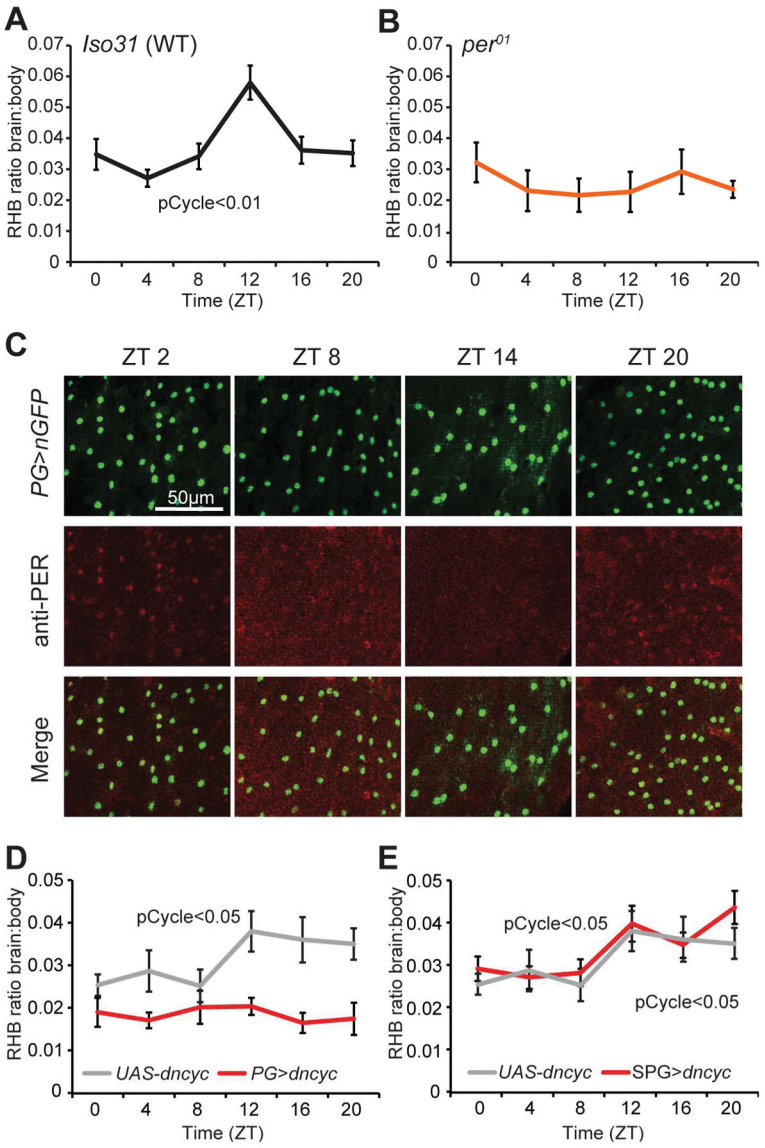


**Figure 1. A circadian clock in the *Drosophila* BBB regulates RHB permeability of the brain**

(a–b) Rhythm of permeability into the *Drosophila* brain: Flies were injected with RHB under $CO_2$ anesthesia at different time points and the levels of RHB in individual fly brains and bodies were measured after 1 hr using a fluorescence reader at Ex540/Em595. The level of RHB fluorescence in the brain was normalized to the amount of RHB in the body to control for injection consistency. Shown are the brain:body ratios of RHB in a) iso31 n=14–21 per time point, pooled from 3+ experiments and b) *per*$^{01}$ flies. n=8–21, pooled from 2 experiments. Means ± SEM are shown. c) Expression of the PER clock protein in the BBB. PG-*GAL4>UAS-nGFP Drosophila* were entrained to a 12:12 LD cycle for 3 days. The brain was analyzed for *nGFP* and PER expression at ZT2, ZT8, ZT14, and ZT20 with a confocal microscope. Representative images of the surface of the brain are shown. Each panel represents an area 100×120μm. (d–e) The PG clock is required for the permeability rhythm. *UAS-dncyc* (control) and d) PG-*GAL4>UAS-dncyc* (experimental) or e) *UAS-dncyc*

(control) and SPG-*GAL4> UAS-dncyc* (experimental) were injected with RHB under $CO_2$ anesthesia and assessed by Ex540/Em595 fluorescence after 60 mins. Means ± SEM of the ratio of brain:body fluorescence are depicted. n=12–22, pooled from 4 experiments. pCycle indicates a presence of rhythm using JTK cycle analysis. See also Figure S1.

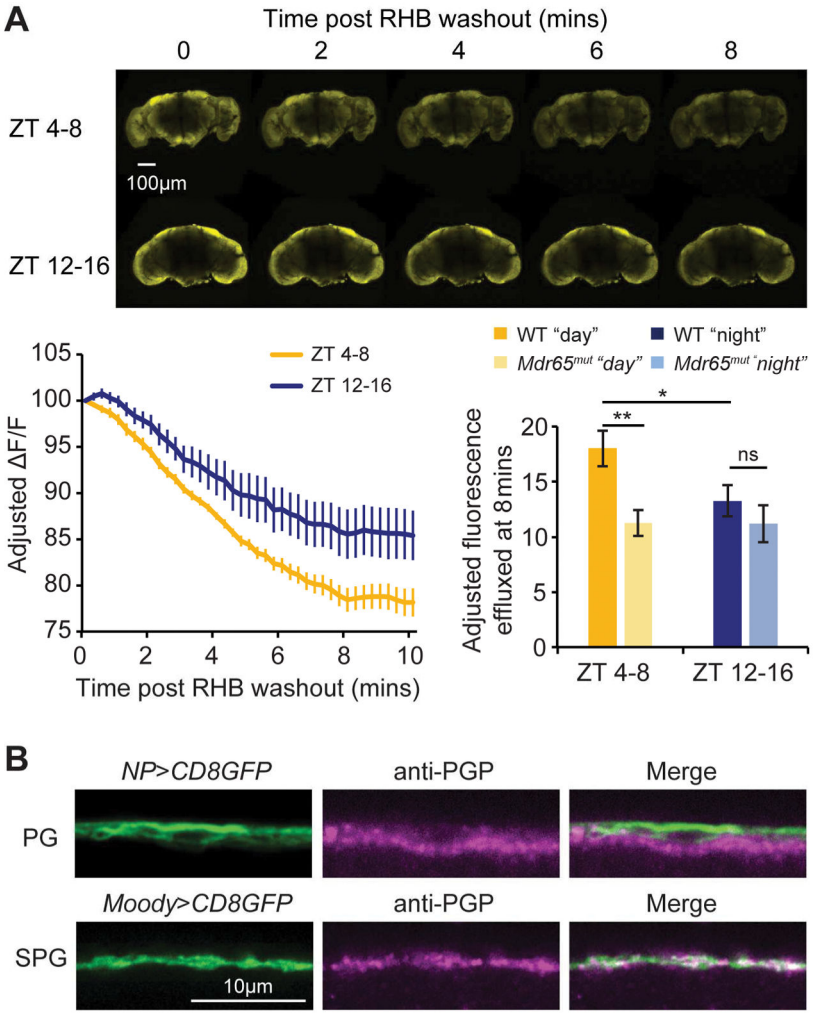


**Figure 2. Pgp-homologous transporters in the SPG regulate diurnal differences in efflux of RHB**

a) Efflux from the *Drosophila* brain. Live brains from wild type or *mdr65*$^{mut}$ flies at ZT4-8 or ZT12-16 were dissected in HL3.1 media and incubated with RHB for 2 mins. Dye was washed off and brains were immediately imaged with a confocal microscope. Representative images are shown (top panel). Adjusted change in fluorescence of live brains over time was quantified for brains assayed at ZT4-8 and at ZT12-16 (bottom left panel); the two samples are compared at 8–9 min time point (bottom right panel). n=9–12 brains, pooled from 4 independent experiments. b) Expression of p-glycoprotein in the BBB. Brains from PG-*GAL4>UAS-mCD8GFP* (top panels) or SPG-*GAL4>UAS-mCD8GFP* (bottom panels) were dissected and incubated with c219 anti-pgp antibody and imaged with a confocal microscope. Pgp expression co-localized with the SPG, but not the PG. Representative images of GFP expression (left), pgp fluorescence (center), and overlay (right) are shown. See also Figure S2.

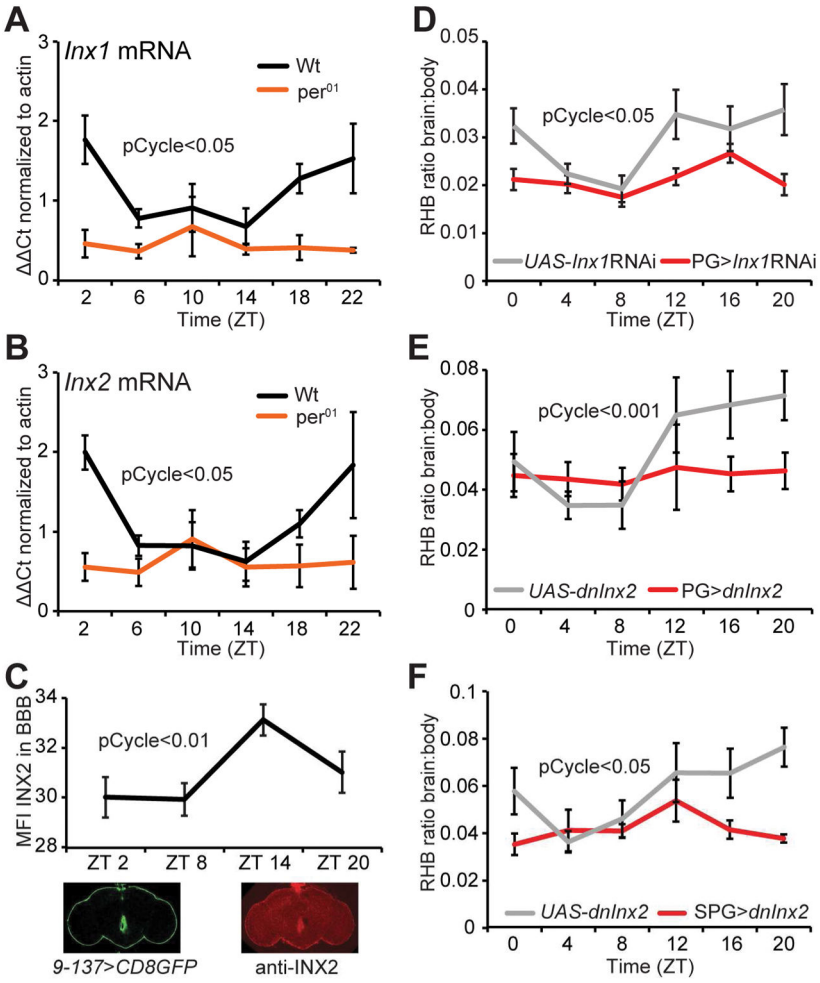


**Figure 3. Circadian signals from the PG to the SPG require gap junctions**

(a–b) Expression of *Inx1* and *Inx2* across the day. Brains from WT and per$^{01}$ flies were dissected and mRNA levels of *Inx1* (left panel) and *Inx2* (right panel) were measured by qPCR. (c) INX2 expression in the BBB. Brains from 9-137-*GAL4>UAS-mCD8GFP* (green) were stained with anti-INX2 antibody (red). Mean fluorescent intensity (MFI) of INX2 colocalized within GFP+ fluorescence was quantified. pCycle indicates a presence of rhythm using JTK cycle analysis. (d–f) Effects of inhibiting gap junctions on the permeability rhythm. PG-*GAL4>UAS-Inx1*$^{RNAi}$ (gd) (d) or PG-*GAL4>UAS-dnInx2* (e) and corresponding genetic control flies were injected with RHB at different time points and the levels of RHB in individual fly brains and bodies were assessed by Ex540/Em595 fluorescence after 1 hr. Means ± SEM of the ratio of brain:body are shown. n=10–22, pooled from 2+ experiments. pCycle indicates a presence of rhythm using JTK cycle analysis. SPG-*GAL4>UAS-dnInx2* (f) and corresponding genetic control flies were injected with RHB at different time points and the levels of RHB in individual fly brains and bodies were assessed by Ex540/Em595 fluorescence after 1 hr. Means ± SEM of the ratio of brain:body are shown. n=9–17, pooled from 3 experiments. pCycle indicates a presence of rhythm using JTK cycle analysis. See also Figure S3.

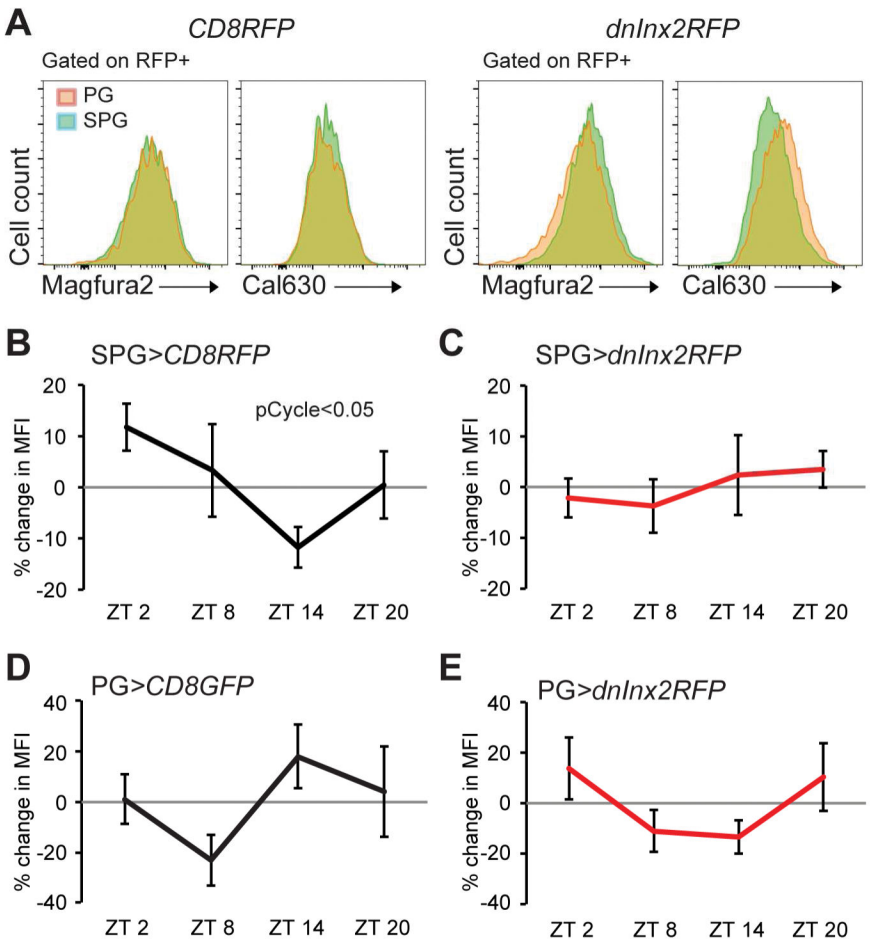


**Figure 4. Functional gap junctions are necessary for [$Mg^{2+}$]i cycling in the SPG**

a) Expression of magnesium and calcium in BBB layers. Dissected brains from PG-*GAL4>UAS-mCD8RFP*, SPG-*GAL4>UAS-mCD8RFP*, PG-*GAL4>UAS-dnInx2RFP*, or SPG-*GAL4>UAS dnInx2RFP* were incubated with [$Mg^{2+}$]i indicator and [$Ca^{2+}$]i indicator, dissociated, and analyzed by flow cytometry. n=3 from 3 independent experiments. Representative plots are shown. (b–e) Effects of blocking gap junctions on magnesium rhythms in the PG and SPG. b) SPG-*GAL4>UAS-mCD8RFP*, c) SPG-*GAL4>UAS-dnInx2RFP*, d) PG-*GAL4>UAS-mCD8GFP*, or e) PG-*GAL4>UAS-dnInx2RFP* from brains at ZT2, ZT8, ZT14, ZT20 were incubated with [$Mg^{2+}$]i indicator dissociated, and analyzed by flow cytometry. The percent changes in mean fluorescent intensity (MFI) of the indicator is shown as means ± SEM. n=4 from 3 experiments. pCycle indicates a presence of rhythm using JTK cycle analysis. See also Figure S4.

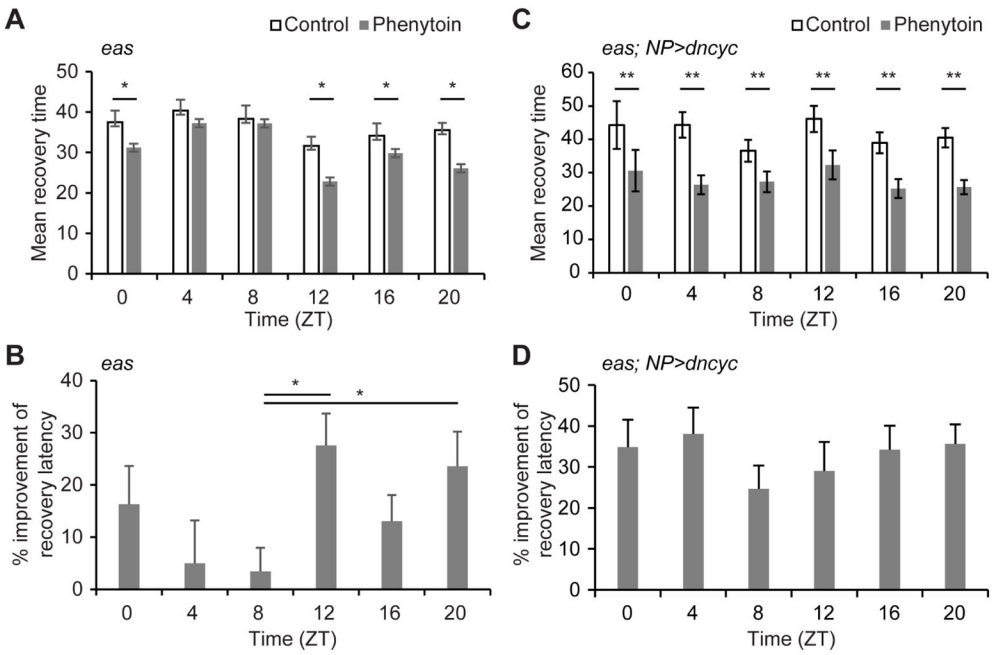


**Figure 5. Effect of phenytoin on seizure mutants is dependent on the clock**

15–20 *eas* mutants were entrained to a 12:12 LD cycle for >3 days, starved for 24 hrs, and fed vehicle or phenytoin for 2 hrs in agar vials. Seizures were induced by mechanical stimulation and the number of seizing flies was counted every 15 secs to calculate mean recovery for each vial. a) Means ± SEM of average recovery latency for each vial, *p<0.05 between vehicle-treated vials and phenytoin-treated vials, shown by paired Student's t-test. b) Means + SEM of the percentage difference in recovery latency between vehicle and phenytoin are shown. Statistical analysis was performed with one-way ANOVA with post-hoc multiple comparisons Tukey test *p<0.05. c) 15 *eas* mutants with *NP6293-GAL4>UAS-dncyc* were entrained and fed vehicle or phenytoin as described above. Means ± SEM are shown. **p<0.01 between vehicle-treated vials and phenytoin-treated vials are shown by Student's t-test. d) Means + SEM of the percentage difference in the recovery latency between vehicle and phenytoin. Unfortunately we are unable to directly compare recovery times of *eas* mutants with *eas* mutants carrying PG-*GAL4>UAS-dncyc* due to the differences in seizures and kinetics of recovery. All time points of the *eas* mutants with PG-*GAL4>UAS-dncyc* at baseline (without drug) had greater mean recovery time, but fewer seizing flies. See also Figure S5.

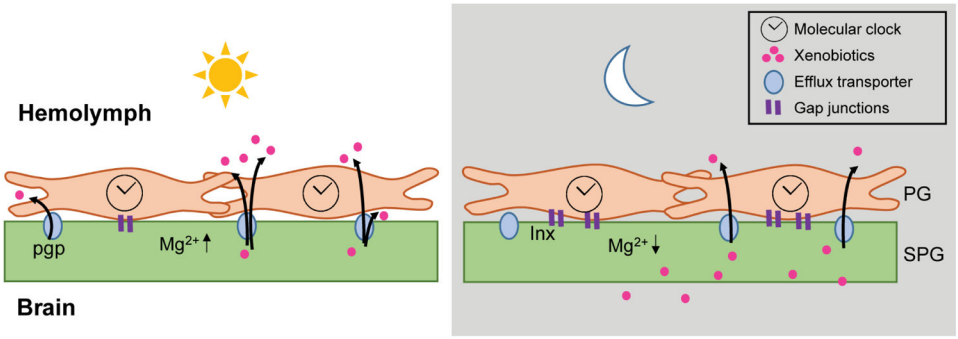


**Figure 6. Model of circadian regulation of BBB efflux**

During the day, circadian clock regulation in the PG lowers levels of gap junctions, reducing connectivity with the SPG. The level of $[Mg^{2+}]i$ is high in the SPG, which promotes activity of the efflux transporters, reducing permeability of xenobiotics. During the night, the PG clock increases gap junctions, thereby increasing connectivity with the SPG. The $Mg^{2+}$ ions diffuse from SPG into the PG, lowering the $[Mg^{2+}]i$ in the SPG. The efflux transporters have reduced activity due to the decline in $[Mg^{2+}]i$ and xenobiotics are retained in the brain.